Air pollution reductions caused by the COVID-19 lockdown open up a way to preserve the Himalayan Glaciers

Suvarna Fadnavis[1*], Bernd Heinold[2], T. P Sabin[1], Anne Kubin[2], Katty Huang[3], Alexandru Rap[4], and Rolf Müller[5]

[1]Indian Institute of Tropical Meteorology, Centre for climate change research, Ministry of Earth Sciences, India

[2]Leibniz-Institut für Troposphärenforschung, Leipzig, Germany,

[3]Urban Climate, Risk & Health, UCL, London, United Kingdom

[4]School of Earth and Environment, University of Leeds, Leeds, UK,

[5]Forschungszentrum Jülich GmbH, IEK-7, Jülich, Germany,

Corresponding author email: suvarna@tropmet.res.in

Abstract

The rapid melting of glaciers in the Hindu Kush Himalayas (HKH) during recent decades poses an alarming threat to water security for larger parts of Asia. If this melting persists, the entire Himalayan glaciers are estimated to disappear by end of the 21st century. Here, we assess the influence of the spring 2020 COVID-19 lockdown on the HKH, demonstrating the potential benefits of a strict emission reduction roadmap. Chemistry-climate model simulations, supported by satellite and ground measurements, show that lower levels of gas and aerosol pollution during lockdown led to changes in meteorology, and to a reduction in black carbon in snow (2-14%) and thus in snow melting (10-40%). This caused increases in snow cover (6-12%) and mass (2-20%) and a decrease in runoff (5-55%) over the HKH and Tibetan Plateau, ultimately leading to an enhanced snow-equivalent-water (2–55%). We emphasize the necessity for immediate anthropogenic pollution reductions to address the hydro-climatic threat to billions of people in South Asia.

1. Introduction

The Hindu Kush Himalayan (HKH) mountains and Tibetan plateau is the largest snow-cladded region outside the Poles (Fig. 1). This region is also referred to as High Mountain Asia, although that includes the Tien Shan and some other northern ranges. The HKH meltwater feeds rivers in India and China that drive the agriculture, hydropower generation, and economy of these countries (Hussain et al., 2019; Sabin et al., 2020; Lee et al. 2021a). The Himalayan snowmelt in spring provides ~50% of the annual freshwater to ~4 billion people of South Asia and East Asia (Sarangi et al 2019, Sabin et al., 2020). Rapid Himalayan snowmelt caused a loss of ~40 % of the Himalayan glacier area compared to the Little Ice Age, 400 to 700 years ago, i.e. ~0.92 to 1.38 mm sea-level equivalent (Lee et al., 2021b). The snow mass over the Himalayas has generally decreased during the last 30 years (except for a few Karakoram glaciers that show an increasing trend in snow mass) (Hussain et al., 2019. The alarming rate of snow melting of 0.02 to 0.6 cm $^{o}C^{-1}$ day^{-1} raised concerns about the sustainability of water supply (Tiwari et al., 2015) and loss of glaciers in the region (Hussain et al., 2019, Lee et al., 2021b). Model simulations for extreme scenarios show that Himalaya snow melting could cause the glaciers to disappear by the end of the 21st century (Cruz et al. 2007, Hock et al., 2019).

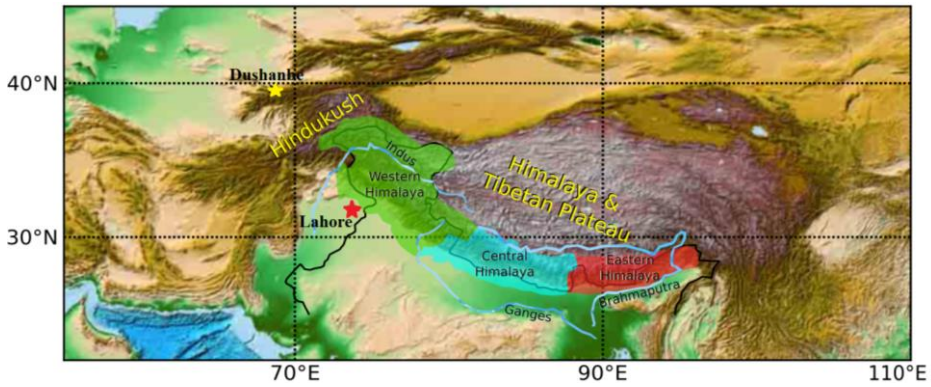

Figure 1: Map of the Hindu Kush Himalayas region with the Western (70 - 80º E, 30º - 35º N), Central (80º - 87º E, 28º - 30º N), and Eastern Himalayas (88º - 95º E, 26º - 30º N). A yellow and red star indicates the location of the AERONET sun photometer stations Dushanbe (68.858º E, 38.553 º N) and Lahore (74.264º E, 31.480º N), respectively.

The accelerated thinning of Himalayan glaciers is attributed to climate change causing shifts in air temperature and precipitation, as well as the atmospheric distribution and deposition of light-absorbing particles i.e., dust and black carbon (BC) (IPCC Climate Change 2013, Krishnan et al., 2019). Among the aforementioned factors, snow darkening due to the deposition of absorbing aerosols is an integral component of Himalayan snowmelt and runoff (Lau et al., 2010). The snow-melting efficacy of BC is higher than that of greenhouse gases (Qian et al., 2011; Nair et al. 2013; Ma et al., 2019; Sarangi et al., 2019). The increasing energy demand of the densely populated South Asian region has increased the emission of greenhouse gases and BC aerosol in the last few decades (Fadnavis et al., 2017, Krishnan et al., 2020), leading to enhanced darkening and snow melting (Usha et al., 2021).

The economic slowdown caused by the COVID-19 pandemic measures led to a drastic reduction in public and freight transportation, industrial emissions, and energy use (Fadnavis et al., 2021a). This resulted in a substantial decline in emissions of several atmospheric pollutants including greenhouse gases and black carbon aerosol (Forster et al. 2020; Kanniah et al., 2020; Le Quéré et al 2020), and potentially reduced deposition of dark aerosols on snow and ice (Bair et al., 2021). Remote sensing approaches show cleaner snow with ~30% less light-absorbing impurities in snow during the lockdown period over Asia between March and May 2020 (Bair et al 2021). This led to decreased snowmelt by 25 – 70 mm in 2020 compared to the last 20-year mean for March-May over Western Himalayas due to decreased radiative forcing induced by BC and dust deposition on snow/ice surfaces and related changes in snow absorption and surface albedo (Bair et al., 2021). Bair et al. (2021) also found that 6.6 km^{-3} of melt water stayed in the Indus Basin. Gauge and reservoir data for this part of the world, however, are not freely available. Impacts of reduced levels of air pollution on changes in the snow mass, surface water runoff, and water reservoir over the HKH are not reported hitherto.

Here, we provide a detailed analysis of the impact of reduced pollution over HKH and Tibetan plateau region during the COVID-19 lockdown period between March and May 2020. We used global simulations with the chemistry-climate model ECHAM6-HAMMOZ (Schultz et al., 2018, Tegen et al., 2019), updated with an improved BC-in-snow parameterization (Huang 2018), in order to contrast the 2020 COVID-19 (COVID) with the typical, unchanged (control, CTL) air pollution conditions. The COVID simulations are performed using a COVID-19 emission inventory where emissions are reduced based on Google and Apple mobility data (Forster et al., 2020; details in section 2.2).

2. Methods

2.1 Observational data

We used monthly snow cover fraction from NASA's Moderate Resolution Imaging Spectroradiometer (MODIS) satellite product on a 0.5x0.5° resolution (version 6, level 3; Hall et al., 2006) for the years 2000 – 2020 (https://nsidc.org/data/MOD10CM/versions/6). For aerosol information we used monthly mean satellite AOD at 1x1° resolution from the MODIS Terra level-3 dark target and deep blue retrievals at 550 nm wavelength for 2001-2020 (https://giovanni.gsfc.nasa.gov). Uncertainty in MODIS AOD data over snow are documented by Huang et al (2020). We also used ground-based sun photometer observations of AOD from the Aerosol Robotic Network (AERONET) (Martonchik et al., 2004) at the stations Dushanbe (68.858º E, 38.553º N) for the period 2010-2020 and Lahore (74.264º E, 31.480º N) for the period 2006 – 2020, situated in HKH region (https://aeronet.gsfc.nasa.gov).

2.2 The ECHAM6-HAMMOZ model description and Experimental set-up

We performed 10-member ensemble experiments using the state-of-the-art aerosol-chemistry-climate model ECHAM6-HAMMOZ (version echam6.3-ham2.3-moz1.0; Schultz et

al., 2018, Tegen et al., 2019). The model comprises the atmospheric general circulation model ECHAM6 (Stevens et al., 2013), the atmospheric chemistry module MOZ (Schultz et al, 2018), and the Hamburg Aerosol Model (HAM; Stier et al., 2005; Zhang et al., 2012). The HAM component predicts the nucleation, growth, evolution, and sinks of sulphate (SO_4^{2-}), black carbon (BC), particulate organic matter (POM), sea salt (SS), and mineral dust (DU) aerosols. Seven log-normal modes describe the size distribution of the aerosol population with a prescribed variance in the aerosol module. The MOZ submodule describes the trace gas chemistry from the troposphere to the lower thermosphere. The chemical mechanism includes the O_X, NO_X, HO_X, ClO_X and BrO_X chemical families, along with CH_4 and its degradation products. Several primary non-methane hydrocarbons (NMHCs) and related oxygenated organic compounds are also described. It contains 108 species, 71 photolytic processes, 218 gas-phase reactions and 18 heterogeneous reactions with aerosol (Schultz et al., 2018). Details of emissions (anthropogenic, biomass burning, biogenic, fossil fuel etc.) and model parametrisation and other details are reported in the past Fadnavis et al. (2017, 2019a,b, 2021b). Anthropogenic and biomass burning emissions of sulphate, and black carbon (BC) and organic carbon (OC) are based on the AEROCOM-ACCMIP-II emission inventory for year 2020 (Lamarque et al., 2010; Textor et al., 2006). Additional consideration for the reduction of snow albedo due to BC in snow is implemented but extended for the MOZ module. The model also accounts for changes in snow albedo due to airborne BC deposited in the top layer of snow, while the effect of other in-snow aerosol particles (e.g. dust, OC) is not simulated in the model. Influxes of BC in snow include below-cloud and in-cloud wet scavenging, as well as dry deposition and sedimentation. Snowmelt and glacier runoff remove the in-snow BC at a reduced efficiency, leading to enhanced concentration, while fresh and pristine snowfall leads to reductions in BC concentration.

The model simulations were performed at T63 horizontal resolution (1.875°× 1.875°) with 47 levels in the vertical from the surface to 0.01 hPa (corresponding to approx. 80 km), and with a time step of 20 minutes. To understand the effect of the COVID-19 restrictions on snow over Himalayas and Tibetan plateau region we conducted a control (CTL) and a COVID-19 (COVID) simulation. We adopted an ensemble approach (with 10 ensemble members) for the above two experiments. Ten spin-up simulations were performed from 1 to 31 December 2019 to generate stabilised initial fields for the 10 ensemble members. Emissions were the same in each of the 10 members during the spin-up period. Control simulations were extended with the same setup until 1 June 2020. While for the COVID simulations (10 ensemble members each), the anthropogenic emission of all gases and aerosols were changed since 1 January 2020 according to Google and Apple mobility data as in Forster et al. (2020). The COVID-19 emissions were prepared by deriving scaling factors between the input4MIPS SSP245 baseline and the version5 of the Forster et al. (2020) 2-year blip scenario, separately for each species and each grid point (see Fig. S5a). Subsequently, these scaling factors have been applied to the AeroCom-II ACCMIP emissions. This ensures consistency of the drop in emissions independent of the absolute emission values in the AeroCom-II ACCMIP and the input4MIPS SSP245 data sets. The global mean emission changes in carbon monoxide (CO, 2-24%), black carbon (BC, 3-23%), organic carbon (OC, 2-17%), sulfur dioxide (SO_2, 3-23%), nitrogen o xides (NO_x, 2-30%), methane (CH_4, 2-5%), and ammonia (NH_3, 0-3%) during the period January to 1 July 2020 (COVID - CTL) are in agreement with previous studies Forster et al. (2020) and Le Quéré et al., (2020) (Fig. S5b). Our model experiments follow the CovidMIP protocol (Jones et al., 2021). The COVID and CTL simulations ended on 1 June 2020. To investigate the effects of COVID-19 emissions in spring (i.e., since 1 March 2020), we analysed the difference between COVID and CTL simulations for the spring season in 2020. The same dust parametrisation was employed in the CTL and COVID simulations.

A limitation of our simulation is the relatively coarse spatial resolution in the ECHAM6-HAMMOZ model (1.875°x1.875°). Other studies used a finer spatially resolved regional model; for example Sarangi et al. (2020) use a 12 x 12 km (~ 0.10°) grid in the regional WRF-Chem-SNICAR model over the same region. In our model grid of 1.875°, many of the Himalayan sub ranges are smaller than a pixel, and, hence, the topographic influences, which are substantial in the mountains are limited. One effect may be that snowfall and snow on the ground are underestimated (e.g., Liu et al., 2022). The coarse grid size can impact the anomalies found here as the changes in snow mass are small, at most +16 mm, and the bias in the likely underestimated snow mass may change between the control and COVID simulations. Biases are, however, the same in the control and COVID simulations and, thus, their effects will be diluted when we compute the anomalies.

3 Comparison of AOD over Western, Central, Eastern Himalayas and Tibetan Plateau regions

We elaborate on the comparison of MODIS AOD with our model simulations over Western, Central, Eastern Himalayas and Tibetan Plateau regions (Fig. S6). Both MODIS and the model show a reduction in AOD during spring 2020 over the aforementioned regions of HKH. The estimated differences in AOD during March to May 2020 vary between 0.8 – 11% over Western and Central Himalayas, and 8 – 16% over Eastern Himalayas. Over the Tibetan plateau region, in contrast to the model simulations, MODIS shows an enhancement (2 – 16 %) in AOD (Fig. S6). This may be due to dust aerosols, which are transported during spring from western Asia and locally, generating dust piles over the Tibetan Plateau (Fadnavis et al., 2017, 2021a). The simulated dust aerosol concentration in spring 2020 over the Tibetan Plateau region is smaller in the COVID than in the non-COVID (i.e. CTL) situation (Fig. S1c). The changes in simulated dust are a response to meteorology differences between the COVID and CTL simulations (Fig. S7).

4 Results

4.1 Reduction of airborne aerosols and in-snow BC concentration over the Himalayas

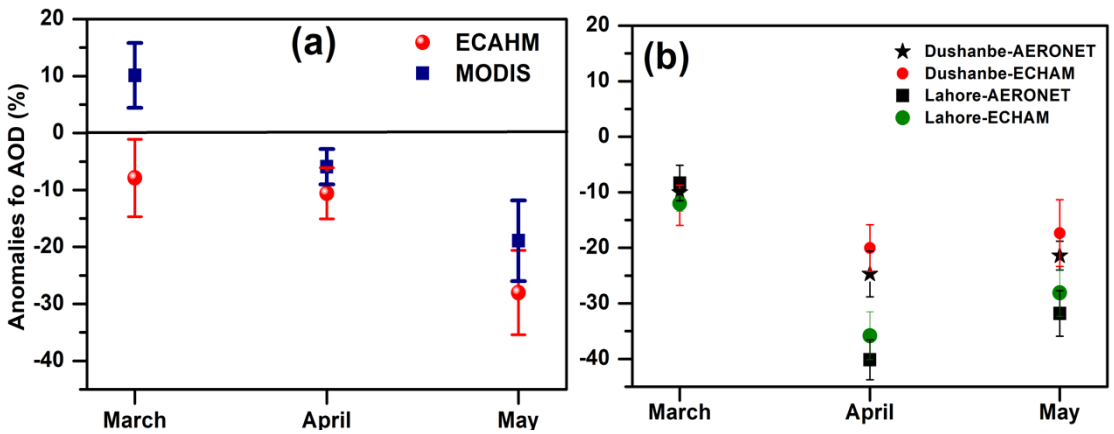

Figure 2: (a) Changes in monthly mean AOD (%) during March - May 2020 from MODIS in comparison to mean of 2001-2019 and ECHAM-HAMMOZ (COVID minus CTL) averaged over the Hindu Kush Himalayas (HKH) and Tibetan Plateau region (75º - 95º E, 30º - 35º N), (b) same as (a) but for AOD from AERONET observations and ECHAM-HAMMOZ model results at Dushanbe (68.858º E, 38.553º N, climatology 2010-2019) and Lahore (74.264º E, 31.480º N, climatology 2006-2019). Vertical bars in Fig (a)-(b) indicate the standard deviation within ten members of model simulations, and within monthly mean anomalies from MODIS for years 2001-2019.

The COVID-19 lockdown restrictions in spring 2020 decreased the anthropogenic aerosol amounts over the HKH ranges (Western, Central, and Eastern Himalayas), and the Tibetan Plateau region. The ECHAM6-HAMMOZ model simulations show that COVID lockdown resulted in a cleaner atmosphere during March - May 2020 over the HKH ranges and Tibetan Plateau region. There is a reduced level of Aerosol Optical Depth (AOD) over the region throughout spring 2020 by -8.1±6.2 % in March, -10.2±4.7% in April, -27±6.9 % in May compared to the CTL (non COVID) simulation (Fig. 2a). This is supported by NASA's Moderate Resolution Imaging Spectroradiometer (MODIS) measurements also showing a reduction in AOD in April (-5.6±3.3%) and May (-18.8±7.2%) 2020 compared to the mean over the last 20 years (Fig. 2a). Thus, both model simulations and MODIS AOD show a reduction in aerosol pollution in April - May 2020. For March 2020, MODIS measurements

show AOD enhancement by 10.2 ±4.8 %, which is due to increased dustiness over the HKH region (see section 3 for a detailed discussion). AOD measurements at two Aerosol Robotic Network (AERONET) sun photometer stations in Dushanbe (68.858º E, 38.553º N) and Lahore (74.264º E, 31.480º N) show an AOD reduction in agreement with our model simulations (Fig. 2b). There are differences among MODIS, AERONET and the model. The changes in AOD during COVID compared to no-COVID period is less in the model than the MODIS observations by 4.2 - 9.8 % and higher than the AERONET observations by 1.8 - 4.2 %. These differences are due to the fact that the simulated AOD change is in response to the reduction of anthropogenic aerosols and associated circulation responses, while MODIS and AERONET measurements show the effect of all atmospheric processes. Also, note that the MODIS AOD values are spatial averages representative for a relatively large area while the AERONET values are point measurements. Importantly, changes in simulated AOD in 2020 fall within the standard deviation of satellite and ground-based measurements indicating reliability of our simulations (except for March 2020 with respect to MODIS). Our model simulations also show a reduction in BC burden by 15 - 55% (Fig. S1a), and sulfate burden by 22 - 24 % over the HKH and Tibetan Plateau regions in spring 2020 (Fig. S1b). Interestingly, dust burden also shows a reduction over these regions (Fig. S1c, Fig. S2a-c), except over central Himalaya in March and April 2020. The lower dust load is related to the interactive change in atmospheric dynamics in the model, which also leads to changes in the wet and dry deposition rates of dust (Fig. S2d-i) (details in section 3). A drop in BC is also observed in Aerosol Radiative Forcing Over India Network (ARFINET) ground-based measurements over the Indo-Gangetic Plain (> 50 %), north-eastern India (>30%), Himalaya regions (16 - 60%), and Tibet (70%) during spring 2020 (Gogoi et al., 2021; Liu et al., 2021). A similar impact of the reduction of energy consumptions on decrease in AOD during the COVID-19 lockdown period, i.e., in spring 2020 compared to the 2010-2019 climatology is also seen over South and East

228 Asia (40 %) and the Indo-Gangetic Plain (IGP) by 30 – 40 % in satellite measurements
229 (Fadnavis et al., 2021a; Srivastava et al., 2021; Pandey et al., 2021; Shafeeque et al , 2021).

230

231 The reduction in anthropogenic air pollution leads widely to a reduction in BC
232 concentration in the snow of approximately 25 - 350 µg kg^{-1} (by 12 – 35 %) during spring 2020
233 (Fig. 3a-c) that reduce the snow darkening effect by embedded aerosol impurities. At the most
234 this amounts to about a 1.6% increase in visible snow albedo. Sporadically, however, the BC-
235 in snow concentrations have also increased in some areas of the Hindukush, Eastern Himalayas
236 and Kunlun Mountains. There are many factors at play that may lead to an increase in BC
237 concentration in snow in some locations. For instance, this includes increases in deposition of
238 BC following shifts in the atmospheric circulation (Fig.S3), accumulation of BC on surface
239 snow following partial snowmelt and minimal fresh snowfall, and less frequent occurrences of
240 complete snowmelt which would otherwise remove all accumulated BC in snow. Our
241 simulations reveal that the decrease in BC-in snow concentration and the overall reduction in
242 atmospheric pollution, as well as associated radiative effects, have decreased the shortwave
243 radiative forcing at the surface by 0.2 – 2 W m^{-2} in March – May 2020 (Fig. 3 d-f), leading to
244 a decrease in tropospheric heating by solar radiation of 0.001 to 0.015 K day^{-1} (Fig. 3 g-i). The
245 reduced anthropogenic BC over the HKH and Tibetan Plateau region resulted in less absorption
246 and re-emission of longwave radiation and, as a consequence, there is a reduction in longwave
247 radiative forcing in the atmosphere leading to a lower atmospheric heating (Fig. S4). This
248 decreased heating of the snowpack and tropospheric column is the combined effect of the reductions of
249 BC in snow, as well as changes in atmospheric concentrations of sulfate, OC and BC.

250

251

252

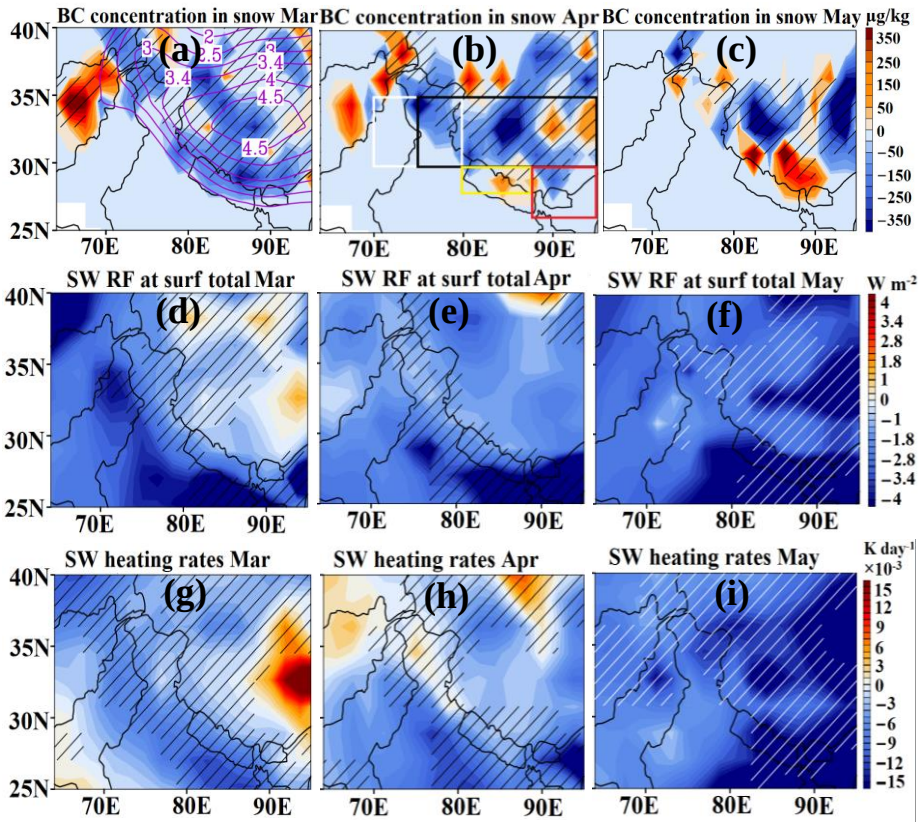

Figure 3: Spatial distribution of anomalies (COVID minus CTL) of BC concentration in snow (µg kg^{-1}) for (a) March, (b) April, and (c) May 2020; (d-f) shortwave radiative forcing (W m^{-2}) at the surface and (e-g) tropospheric heating rates (K day^{-1}) due to changes in BC concentration in snow (COVID minus CTL). Hatched areas indicate the 95%-significance level. Contours in panel (a) indicate topography in km. Boxes in panel (b) indicate boundaries of Western Himalayas (WH, white), Central Himalayas (CH, yellow), Eastern Himalayas (EH, red) and Tibetan Plateau (black).

4.2 Impacts on snow melting, surface water runoff, and snow cover

Further we show that the decrease in aerosol pollution reduced the snow melting in spring 2020 by 0.2 to 2.5 mm day^{-1} corresponding to 10 – 50 % (Fig. 4 a-c). The amount of reduction of snow melting is pronounced over the western Himalayas in May. As a result of a reduction in snowmelt, surface water runoff has been drastically reduced by 2-4 mm $–ay^{-1}$ (5 - 55 %) (Fig. 4 d-f). The reduction in the runoff is most pronounced in May over the entire Himalayas and central Tibetan Plateau region. Estimates from remote sensing measurements also show the reduction of runoff by 6.5 km^3 of melted water in the Indus River Basin (Bair et al. 2020). In the past, studies have shown that elevated levels of light-absorbing aerosols

(elemental carbon: 13 to 75 ng g^{-1} and dust: 32 to 217 μg g^{-1}) can contribute to about 3 to 10 mm day^{-1} of snowmelt over western Himalayas (Thind et al. 2019). A sensitivity analysis by (Santra et al., 2019) using a glacier mass balance model shows that BC-induced snow albedo reduction leads to an increase in annual runoff of 4 – 18%. In contrast to impacts of rising anthropogenic emissions during the past decades, emission reductions during the 2020 COVID-19 lockdown period caused a brighter snow albedo and therefore an enhanced surface reflection with albedo increases of 0.2 – 0.5 (see Fig. 4g-i), leading to less atmospheric heating as well as associated reduced snowmelt and surface water runoff in spring 2020.

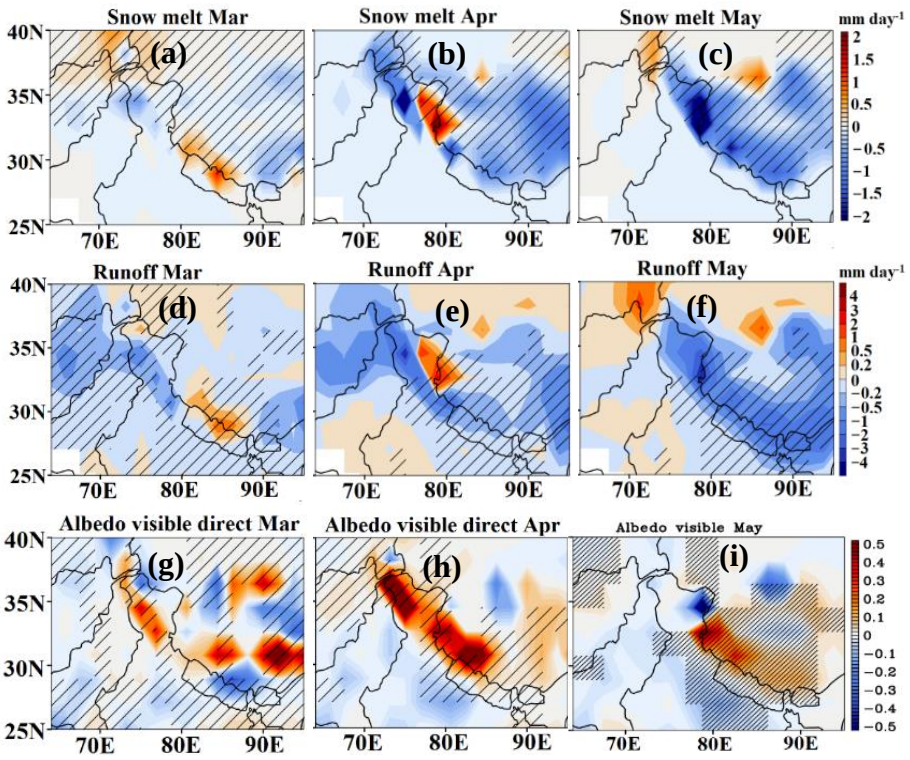

Figure 4: Spatial distribution of anomalies of (a-c) snow melt (mm day^{-1}), (d-f) surface water runoff (mm day^{-1}) for March to May 2020 (COVID minus CTL) and (g-i) surface albedo mean in the visible. Hatched areas indicate the 95%-significance level.

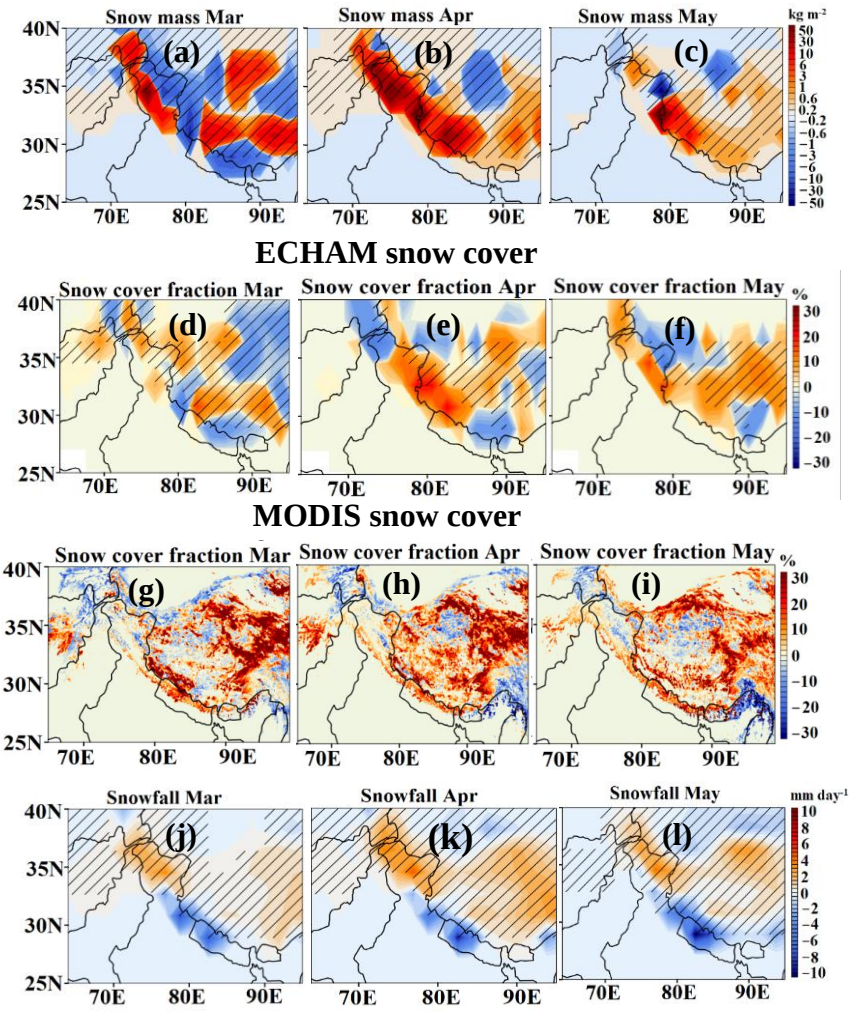

Figure 5: Monthly mean anomalies (COVID minus CTL) for March to May 2020 of (a-c) the snow mass (kg m^{-2}), (d-f) snow cover fraction (%) as modelled by ECHAM6-HAMMOZ as well as (g-i) snow cover fraction from MODIS satellite measurements (%) with respect to the climatological average 2000-2019, and, (j-l) snowfall as modelled by ECHAM6-HAMMOZ. Hatched areas indicate the 95%-significance level.

Our simulations also indicate that these changes lead to an increase in snow mass of 0.2-50 kg m^{-2}, i.e. 10-40% (Fig. 5a-c) and snow cover fraction of 2-30% during spring 2020 (Fig. 5d-f). MODIS measurements also show a remarkable agreement with the model simulations (especially during April - May 2020), with increased snow cover of about 15-30% over the parts of Western Himalayas and Central Himalayas and the Tibetan Plateau region and decreased by 5-12 % over parts of North-East Himalayas especially in April and May 2020 (Fig. 5 g-i). However, there are also some differences in terms of exact regions of snow cover

enhancement or reduction respectively, since the MODIS observations include the influence of real-time meteorology, while meteorology in the model ensemble include internal variability and do not replicate the exact conditions observed by MODIS. Our model simulations show that air pollution reductions in the COVID-19 lockdown period and associated changes in radiative forcing caused changes in the tropospheric circulation and thermodynamics (see Fadnavis et al., 2020 for a detailed analysis). These changes in meteorology have increased snowfall by 2-5 mm day^{-1} (3-20 %) over the Western Himalayas and Tibetan Plateau region (Fig. 5 j-l). The increase in snowfall over these regions will contribute to enhancement in snow mass and snow cover (Fig. 5 a-f) and albedo (Fig. 4 g-i). In a few areas, however, this also contributes to a more efficient BC deposition on snow, as described above (Fig. 3). This BC enrichment in snow at a few places, however, has no influence on the fact that overall the COVID-19 measures reduced the BC-in snow concentration and thus increased the visible snow albedo (see Fig. 4g-i).

Himalaya snow is the largest source of freshwater for South Asia (Bolch et al., 2012). The impact of reduced pollution on the surface water content in the Himalayas from our model simulations is illustrated in Fig. 6a. The snow mass enhancement led to increase the snow equivalent water by 2 to 14.7 mm (2.5 to 55 %). The western Himalayas show the highest increase in snow equivalent water by 14.7 mm (55 %) followed by the Tibetan Plateau by 12 mm (by 22 %) and central Himalayas by 10 mm (by 18%) in April while the Eastern Himalayas show a decrease in March (-1.3 mm; 10 %) and small enhancement in April by 1.1mm (2.3 %) and May 2020 by 1.3 mm (2.7%) due to pollution reduction. Thus, human induced pollution reduction during the COVID-19 lockdown benefitted the HKH in many ways. A schematic shows the COVID-19 lockdown-induced effects in Figs. 6b-c: increased snow surface

reflectivity, reduced snowmelt and surface water runoff, as well as enhanced water content in the reservoir and snow.

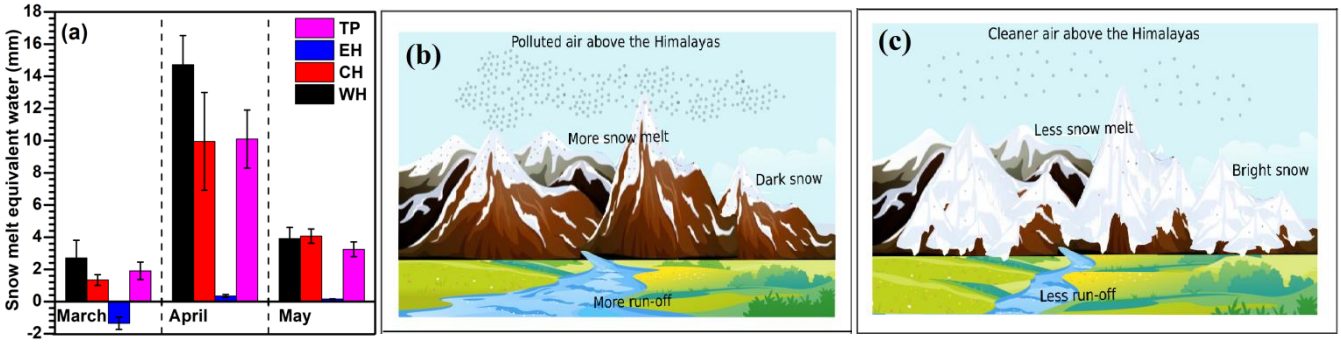

Figure 6: (a) Change in water content (mm) of the Himalayan surface reservoirs (COVID minus CTL) from March to May 2020 over the Western Himalayas (WH), Central Himalayas (CH), Eastern Himalayas (EH) and Tibetan Plateau (TP). Vertical bars indicate the standard deviation within ten members of model simulations. Schematic illustrating the impacts of (b) air pollution on snow darkening in the Himalayas and surface water runoff for the usual polluted case and (c) the impacts of reduced pollution on snow brightening in the Himalayas and reduced surface water runoff, as observed during the 2020 COVID-19 lockdown period.

5 Summary and conclusions

A rising trend in Asian air pollution and associated climate change over the last few decades has had a detrimental impact on snow melting over the Hindu Kush Himalayas (HKH) and Tibetan Plateau region (Wester et al., 2019). Black carbon from increasing emissions of biomass burning, industrial and domestic combustion and transport is deposited on snow, reducing its albedo (i.e. darkening) (Bolch et al., 2019). A snow darkening effect along with pollution reduction, compounded with other climate change effects, accelerates the melting of snow and the disappearance of ice cover over the HKH and Tibetan Plateau region at an extraordinary rate (Usha et al., 2021). The drop in anthropogenic air pollution emissions, e.g. from energy production, during the COVID-19 lockdown period in spring 2020 reduced air pollutant levels worldwide (Forster et al., 2020). Our model simulations indicate that the associated reduction in anthropogenic aerosols and greenhouse gases in spring 2020 has benefited the HKH snow reservoirs. It caused an enhancement in the snow cover fraction by 6 - 12 % and snow mass by 2 - 20 %, corresponding to a decrease in snow melting by 10 - 40% and surface water runoff by 0.2 - 3 mm day^{-1}. As a consequence, the water content of the reservoir increased considerably by 4 to 59 %.

Our findings highlight that out of the two processes causing a retreat of Himalayan glaciers: (1) a slow response to global climate change and (2) a fast response to local air pollution (especially black carbon), a policy action on the latter is more likely to be within reach of possible policy action on a shorter-term time scale and a more regional spatial scale. Even if we stopped CO_2 emissions immediately, temperatures would not start decreasing. Our findings confirm the importance of reducing short-lived climate forcers (black carbon) and their complementary role to CO_2 mitigation (Rogelj et al., 2014). Reduction of air pollution to levels similar with those recorded during the 2020 COVID-19 lockdown period, could safeguard HKH glaciers, which are otherwise under the threat to disappear by the end of the 21st century. Since 2000 Himalayan glaciers have been losing nearly half a meter of ice per year (Wester et al., 2019). Our estimates indicate that air pollution reduction during COVID 19 lockdown in spring 2020 caused a reduction in snow melt by 0.5 to 1.5 mm day^{-1}, indicating large benefits to HKH glaciers. Even if global warming is kept below 1.5°C, one third of the glaciers in the HKH region and more than half of those in the Eastern Himalaya will likely be lost by the end of this century (Bolch et al., 2019). The speedily retreating glaciers and the snowpack loss are already posing a threat to domestic sustainable water resources for billions of people in Asia (Wood et al., 2021). However, if new economically and technically feasible policies would reduce emissions of air pollutants (in particular black carbon) to at least lockdown period levels, snowmelt could be reduced by 10 – 50%. Such policies will therefore bring substantial benefits for sustained water supply, agriculture, and ecosystems in large parts of Asia.

406 References:

407 Bair, E., Stillinger, T., Rittger, K. & Skiles, M. COVID-19 lockdowns show reduced pollution
408 on snow and ice in the Indus River Basin. *Proc. Natl. Acad. Sci. U. S. A.* 118, 19–21,
409 https://doi.org/10.1073/pnas.2101174118, 2021. Bolch, T. *et al.* Status and Change of
410 the Cryosphere in the Extended Hindu Kush Himalaya Region. in The Hindu Kush
411 Himalaya Assessment: Mountains, Climate Change, Sustainability and People (eds.
412 Wester, P., Mishra, A., Mukherji, A. & Shrestha, A. B.) 209–255 (Springer International
413 Publishing). doi:10.1007/978-3-319-92288-1_7 2019, 2019.

414 Cruz, R.V., Harasawa, H., Lal, M., Wu, S, Anokhin, Y., Punsalmaa, B., Honda, Y., Jafari, M.,
415 Li, C., and Huu Ninh, N. Climate change 2001: impacts, adaptation, and vulnerability.
416 *Choice Rev. Online* 39, 39-3433-39–3433, 2007.

417 Fadnavis, S. Müller R., Chakraborty T., Sabin T. P., Laakso A., Rap A., Griessbach S., Vernier
418 J-P. & Tilmes S. The role of tropical volcanic eruptions in exacerbating Indian droughts.
419 *Sci. Rep.* 11, 1–13, https://doi.org/10.1038/s41598-021-81566-0, 2021.

420 Fadnavis, S., Müller R., Kalita G, Rowlinson M., Rap A., Frank Li J-L, Gasparini B, and
421 Laakso A., The impact of recent changes in Asian anthropogenic emissions of SO2 on
422 sulfate loading in the upper troposphere and lower stratosphere and the associated
423 radiative changes, ACP, 19, 9989–10008, 2019a.

424 Fadnavis, S., Sabin T. P., Roy C., Rowlinson M, Rap A, Vernier J-P.& E. Sioris C. E.. Elevated
425 aerosol layer over South Asia worsens the Indian droughts. Sci. Rep. 9, 1–12,
426 https://doi.org/10.1038/s41598-019-46704-9, 2019b.

427 Fadnavis, S., Kalita, G., Ravi Kumar, K., Gasparini, B. & Li, J. L. F. Potential impact of
428 carbonaceous aerosol on the upper troposphere and lower stratosphere (UTLS) and
429 precipitation during Asian summer monsoon in a global model simulation. *Atmos.*
430 *Chem.Phys.* 17, 11637–11654, https://doi.org/10.5194/acp-17-11637-2017, 2017.

Fadnavis, S.. Sabin T. P, Rap A., Müller R., Kubin A. and Heinold B., The impact of COVID-19 lockdown measures on the Indian summer monsoon. *Environ. Res. Lett.* 16, DOI 10.1088/1748-9326/ac109c, 2021.

Forster, P. M. *et al.* Current and future global climate impacts resulting from COVID-19. *Nat.Clim. Chang.* 10, 913–919, 2020.

Gogoi, M. M. S. Babu S., Arun B. S., Krishna, Moorthy K., Ajay A., Ajay P., Suryavanshi A., Borgohain A., *et al.* Response of Ambient BC Concentration Across the Indian Region to the Nation-Wide Lockdown: Results from the ARFINET Measurements of ISRO-GBP.*Curr. Sci.* 120, 341, doi: 10.18520/cs/v120/i2/341-351, 2021.

Hall, D. K. MODIS / Terra Snow Cover 5-Min L2 Swath 500m. *Color. USA NASA Natl. Snow Ice Data Cent. Distrib. Act. Arch. Cent* 5, 2006.

Hock, R. *et al.* Chapter 2: High Mountain Areas. IPCC Special Report on the Ocean and Cryosphere in a Changing Climate. *IPCC Spec. Rep. Ocean Cryosph. a Chang. Clim.* 131–202, 2019.

Huang, W. T. K. Aerosol effects on climate, with an emphasis on the Arctic. https://doi.org/10.3929/ethz-b-000319114 2018, 2018.

Hussain, A. *Sarangi G.K., Pandit A., Ishaq S., Mamnun N., Ahmad B., Jamil M.K.,* Hydropower development in the Hindu Kush Himalayan region: Issues, policies and opportunities. *Renew. Sustain. Energy Rev.* 107, 446–461, https://doi.org/10.1016/j.rser.2019.03.010, 2019.

IPCC Working Group 1, I. *et al.* IPCC, 2013: Climate Change 2013: The Physical Science Basis. Contribution of Working Group I to the Fifth Assessment Report of theIntergovernmental Panel on Climate Change. *Ipcc* AR5, 1535, 2013.

Jones, C. D., et al. The climate response to emissions reductions due to COVID-19: Initial results from CovidMIP. Geophysical Research Letters, 48, e2020GL091883. https://doi.org/10.1029/2020GL091883, 2021.

Kanniah, K. D., Kamarul Zaman, N. A. F., Kaskaoutis, D. G. & Latif, M. T. COVID-19's impact on the atmospheric environment in the Southeast Asia region. *Sci. Total Environ.*736, 139658, https://doi.org/10.1016/j.scitotenv.2020.1396580048-9697, 2020.

Krishnan, R. *et al.* Assessment of climate change over the Indian region: A report of the ministry of earth sciences (MOES), government of India. Assessment of Climate Change over the Indian Region: A Report of the Ministry of Earth Sciences (MoES), Government of India (Springer Singapore). doi:10.1007/978-981-15-4327-2, 2020.

Krishnan, R., Shrestha, A., Ren, G., Rajbhandari, R., Saeed, S., & Sanjay, J. Unravelling Climate Change in the Hindu Kush Himalaya: Rapid Warming in the Mountains and Increasing Extremes. The Hindu Kush Himalaya Assessment (Springer Singapore). doi:10.1007/978-3-319-92288-1_3, 2019.1 , 2019.

Laakso A. The impact of recent changes in Asian anthropogenic emissions of SO2 on sulfate loading in the upper troposphere and lower stratosphere and the associated radiative changes.. *Atmos. Chem. Phys.* 1–44, https://doi.org/10.5194/acp-19-9989-2019, 2019a.

Lamarque J.-F. , Bond T. C., Eyring V., Granier C., Heil A., Klimont Z., Lee D., Liousse C., Mieville A., Owen B., Schultz M. G., Shindell D., Smith S. J., Stehfest E., Aardenne J. Van, Cooper O. R., Kainuma M., Mahowald N., McConnell J. R., Naik V., Riahi K., and Vuuren D. P. van, Historical (1850-2000) gridded anthropogenic and biomass burning emissions of reactive gases and aerosols: Methodology and application. *Atmos. Chem. p*hys. 10, 7017–7039, https://doi.org/10.5194/acp-10-7017-2010, 2010.

Lau, W. K. M., Kim, M. K., Kim, K. M. & Lee, W. S. Enhanced surface warming and accelerated snow melt in the Himalayas and Tibetan Plateau induced by absorbing aerosols. *Environ. Res. Lett.* 5, doi:10.1088/1748-9326/5/2/025204, 2010.

Le Quéré, C. *Jackson R. B., M Jones M. W., Smith A. J. P., Abernethy S. Andrew R. M. , De-Gol A. J. Willi D. R., Shan Y., Canadell J. G., Friedlingstein P., Creutzig F. and Peters* G. P., Temporary reduction in daily global CO2 emissions during the COVID-19 forced confinement. *Nat. Clim. Chang.* 10, 647–653, https://doi.org/10.1038/s41558-020-0797-x., 2020.

Lee, E., Carrivick1 J. L., Quincey D. J., Cook S. J., ames1 W. H. M., &. Brown L. E., Accelerated mass loss of Himalayan glaciers since the Little Ice Age. *Sci. Rep.* 11, 1–8, https://doi.org/10.1038/s41598-021-03805-8, 2021b.

Lee, S. S., Chu, J. E., Timmermann, A., Chung, E. S. & Lee, J. Y. East Asian climate response to COVID-19 lockdown measures in China. *Sci. Rep.* 11, 1–9, 2021a.

Liu, Y. *Wang Y. , Cao Y., Yang Xi, T Zhang T., Luan M., Lyu D., Hansen A. D. A., Liu B., and* Liu, Y., Fang, Y., Li, D., and Margulis, S. A.: How Well do Global Snow Products Characterize Snow Storage in High Mountain Asia?, Geophysical Research Letters, 49, e2022GL100082, https://doi.org/10.1029/2022GL100082, 2022.

Ma, J. Zhang T., and GUAN X., The dominant role of snow/ice Albedo feedback strengthened by black carbon in the enhanced warming over the Himalayas. *J. Clim.* 32, 5883–5899, https://doi.org/10.1175/JCLI-D-18-0720.s1.2019.

Martonchik, J. V., Diner, D. J., Kahn, R., Gaitley, B. & Holben, B. N. Comparison of MISR and AERONET aerosol optical depths over desert sites. *Geophys. Res. Lett.* 31, 1–4, https://doi.org/10.1029/2004GL019807, 2004.

Nair, V. S. *Babu S. S,, Moorthy K. K., Sharma A. K. , Marinoni A.& Ajai,* Black carbon aerosols over the Himalayas: Direct and surface albedo forcing. *Tellus, Ser. B Chem. Phys. Meteorol.* 468 65, DOI: 10.3402/tellusb.v65i0.19738, 2013.

Pandey, S. K. & Vinoj, V. Surprising changes in aerosol loading over india amid covid-19 lockdown. *Aerosol Air Qual. Res.* 21, 1–12, https://doi.org/10.4209/aaqr.2020.07.0466, 2021.

Qian, Y., Flanner, M. G., Leung, L. R. & Wang, W. Sensitivity studies on the impacts of Tibetan Plateau snowpack pollution on the Asian hydrological cycle and monsoon climate. *Atmos. Chem. Phys.* 11, 1929–1948, doi:10.5194/acp-11-1929-2011, 2011.

Rogelj, J. *Schaefferc M., Meinshausene M.,. Shindell D. T, Harec W., Klimontb Z. , Veldersh G. J. M., Amannb M., and Schellnhuberr H.J.,* Disentangling the effects of CO2 and short lived climate forcer mitigation. *Proc. Natl. Acad. Sci. U. S. A.* 111, 16325–16330, https://doi.org/10.1073/pnas.1415631111, 2014.

Sabin, T., Krishnan, R., Vellore, R., Priya, P., Borgaonkar, H., Singh, B., Sagar, A. Droughts and floods. Climate Change Over the Himalayas. Assessment Of Climate Change Over The Indian Region. doi:10.1007/978-981-15-4327-2_11, 2020.

Santra, S. *Verma1 S., Fujita K, Chakraborty I, Boucher O., Takemura T., Burkhart John F., Matt F, and Sharma M.,* Simulations of black carbon (BC) aerosol impact over Hindu Kush Himalayan sites: Validation, sources, and implications on glacier runoff. *Atmos. Chem. Phys.* 19, 2441–2460, https://doi.org/10.5194/acp-19-2441-2019, 2019.

Sarangi, C. Qian Y., Rittger K., Bormann K.J., Liu Y., Wang H., Wan H., Lin G., and. Painter T.H., Impact of light-absorbing particles on snow albedo darkening and associated radiative forcing over high-mountain Asia: high-resolution WRF-Chem modeling and new satellite observations. *Atmos. Chem. Phys.* 19, 7105–7128, https://doi.org/10.5194/acp-19-7105-2019, 2019.

525 Sarangi, C., Qian, Y., Rittger, K., Ruby Leung, L., Chand, D., Bormann, K. J., and Painter, T.
526 H.: Dust dominates high-altitude snow darkening and melt over high-mountain Asia,
527 Nature Climate Change, 10, 1045-1051, 10.1038/s41558-020-00909-3, 2020.
528 Schultz, M. G., Stadtler S., Schröder S., Taraborrelli D., Franco B., Krefting J, Henrot A. et al.,
529 The chemistry-climate model ECHAM6.3-HAM2.3-MOZ1.0. *Geosci. Model Dev.* 11,
530 1695–1723, https://doi.org/10.5194/gmd-11-1695-2018, 2018.
531 Shafeeque, M. Arshad A., A Elbeltagi A., Sarwar A., Pham Q. B., S Khan S. N., l Dilawar A.
532 & Al-Ansari N., Understanding temporary reduction in atmospheric pollution and its
533 impacts on coastal aquatic system during COVID-19 lockdown: a case study of South
534 Asia.*Geomatics, Nat. Hazards Risk* 12, 560–580,
535 https://doi.org/10.1080/19475705.2021.1885503, 2021.
536 Srivastava, A. K.. *Bhoyar P.D., K* 499 *anawade V. P., Devara P.C. S., Thomas A., Soni V.K.*,
537 Improved air quality during COVID-19 at an urban megacity over the Indo-Gangetic
538 Basin: From stringent to relaxed lockdown phases. *Urban Clim.* 36, 100791,
539 https://doi.org/10.1016/j.uclim.2021.100791, 2021.
540 Stevens, B., Giorgetta M., Esch M., Mauritsen T., Crueger T., Rast S., Salzmann M., Schmidt
541 H., Bader J., Block K., Brokopf R., Fast I., Kinne S., Kornblueh L., Lohmann U., Pincus
542 R., Reichler T., Roeckner E. Atmospheric component of the MPI-M earth system model:
543 ECHAM6. J. Adv. Model. Earth Syst. 5, 146–172, https://doi.org/10.1002/jame.20015,
544 2013.
545 Stier, P., Feichter J., Kinne S., Kloster S., Vignati E., Wilson J., Ganzeveld L., Tegen I., Werner
546 M., Balkanski Y. Schulz M., Boucher O., Minikin A., and Petzold A., Theaerosol-climate
547 model ECHAM5-HAM. *Atmos. Chem. Phys.* 5, 1125–1156, https://doi.org/10.5194/acp-
548 5-1125-2005, 2005.

549 Tegen, I., Neubauer D., Ferrachat S., Siegenthaler-Le Drian C, Bey, I., Schutgens N., Stier P.,
550 Watson-Parris D., et al., The global aerosol-climate model echam6.3-ham2.3 -Part 1:
551 Aerosol evaluation. *Geosci. Model Dev.* 12, 1643–1677, https://doi.org/10.5194/gmd-12-
552 1643-2019, 2019.
553 Textor , Schulz M, Guibert S., Kinne S., Balkanski Y., Bauer S., Berntsen T., Berglen T.,
554 Boucher O., Chin M., Dentener F, Diehl1 T., Easter R., Feichter H., Fillmore D., Ghan
555 S., Ginoux P., Gong S., Grini A., Hendricks J. , Horowitz L., Huang P., Isaksen I., Iversen
556 I, Kloster S., Koch D., Kirkevåg A., Kristjansson J. E., Krol M., Lauer A., Lamarque J.
557 F., Liu X., Montanaro V., Myhre G., Penner J., Pitari G., Reddy5 S., Seland Ø., Stier P.,
558 Takemura T., and Tie X., Analysis and quantification of the diversities of aerosol life
559 cycles within AeroCom. *Atmos. Chem. Phys.* 6, 1777–1813, https://doi.org/10.5194/acp-
560 6-1777-2006, 2006.
561 Thind, P. S., Chandel, K. K., Sharma, S. K., Mandal, T. K. & John, S. Light-absorbing
562 impurities in snow of the Indian Western Himalayas: impact on snow albedo, radiative
563 forcing, and enhanced melting. *Environ. Sci. Pollut. Res.* 26, 7566–7578,
564 https://doi.org/10.1007/s11356-019-04183-5, 2019.
565 Tiwari, S., Kar, S. C. & Bhatla, R. Snowfall and Snowmelt Variability over Himalayan Region
566 in Inter-annual Timescale. *Aquat. Procedia* 4, 942–949,doi:
567 10.1016/j.aqpro.2015.02.118, 2015.
568 Usha, K. H., Nair, V. S. & Babu, S. S. Effect of aerosol-induced snow darkening on the direct
569 radiative effect of aerosols over the Himalayan region. *Environ. Res. Lett.* 16,
570 https://doi.org/10.1088/1748-9326/abf190, 2021.
571 Wester P., Mishra A., Mukherji A., S. A. B. The Hindu Kush Himalaya Assessment—
572 Mountains, Climate Change, Sustainability and People. Springer Nature Switzerland AG,
573 Cham. doi:https://doi.org/10.1007/978-3-319-92288-1, 2019.

Wood, L. R. Neumann K., Nicholson K.N., Bird B.W., Dowling C. B. and Sharma *S.*. Melting Himalayan Glaciers Threaten Domestic Water Resources in the Mount Everest Region, Nepal. *Front. Earth Sci.* 8, 1–8, https://doi.org/10.3389/feart.2020.00128, 2020.

Zhang, K. O'Donnell D., Kazil J., Stier P., Kinne S., Lohmann U., Ferrachat S., Croft B., Quaas J, Wan H., Rast S., and Feichter J., The global aerosol-climate model ECHAMHAM, version 2: Sensitivity to improvements in process representations. *Atmos. Chem.Phys.* 12, 8911–8949, https://doi.org/10.5194/acp-12-8911-2012, 2012.

Zheng M.,Impacts of COVID-19 on Black Carbon in Two Representative Regions in China: Insights Based on Online Measurement in Beijing and Tibet. *Geophys. Res. Lett.* 48, 1–11, 10.1029/2021GL092770, 2021.

Acknowledgments

The authors thank the staff of the High Power Computing Centre (HPC) in IITM, Pune, India, for providing computer resources and the team members of MODIS for providing data. We thank Sabur F. Abdullaev and Brent Holben for their efforts in establishing and maintaining Dushanbe and Lahore AERONET sites respectively. Work done in the manuscript is not supported by any funding agency.

Funding information

The manuscript is not funded.

Author Contributions

S.F. initiated the idea of the study. S.F. and B. H. performed model simulations. A.R. and A. K. prepared Google based emission inventory. T.P.S., A.A., R.M. performed data analysis and contributed in overall design. All authors contributed to discussions of the results and the writing of the manuscript.

Data and code availability

The ECHAM-HAMMOZ model source code and all required input data are available to the scientific community according to the HAMMOZ Software License Agreement through the project website: https://redmine.hammoz.ethz.ch/projects/hammoz. The data that support the findings of this study are openly available in zenodo at http://doi.org/.../zenodo....

Competing Interests: The authors declare no competing interests.